

Ti-clinohumite in the Ciénaga skarn-type mineralogy, Sierra Nevada de Santa Marta Massif (Colombia):
Occurrence and petrologic significance

Carlos Alberto Ríos R.^{1*}, Oscar Mauricio Castellanos A.², Carlos Alberto Chacón Avila³

¹Grupo de Investigación en Geología Básica y Aplicada (GIGBA), Escuela de Geología, Universidad Industrial de Santander, Bucaramanga, Colombia, e-mail: carios@uis.edu.co

²Grupo de Investigación en Geofísica y Geología (PANGEA), Programa de Geología, Universidad de Pamplona, Colombia

³Grupo de Investigación en Óptica y Procesamiento de Señales (GOTS), Escuela de Física, Universidad Industrial de Santander, Bucaramanga, Colombia

ABSTRACT

This study reports the occurrence and petrologic significance of Ti-clinohumite for the first time in the Ciénaga skarn, Sierra Nevada de Santa Marta Massif. Ti-Clinohumite occurs as thin bands hosted in the Ciénaga Marbles of lower Cretaceous age, which consist of quartz-wollastonite-diopside-garnet-clinohumite marbles. We focus the attention on the occurrence of Ti-clinohumite-bearing domains, highlighting some interesting textures as well as the mineralogy and chemistry of the Ti-clinohumite. On the basis of its geologic situation, petrography, mineral composition and metamorphic history, we discuss the origin of Ti-clinohumite.

Key Words: Ti-clinohumite; marbles; Ciénaga skarn; mineralogy; Sierra Nevada de Santa Marta Massif.

RESUMEN

El estudio reporta la presencia y el significado petrológico de Ti-clinohumita por primera vez en mármoles del depósito de skarn de Ciénaga, Macizo Sierra Nevada de Santa Marta, de edad Cretácico inferior. La Ti-clinohumita ocurre como bandas delgadas en mármoles de cuarzo-wollastonita-diópsido-granate-clinohumita. Centramos la atención en la ocurrencia de los dominios con Ti-clinohumita, destacando algunas de sus texturas interesantes, así como la mineralogía y la química de la Ti-clinohumita. Con base al contexto geológico, a las características petrográficas, a la composición mineral y a la historia metamórfica, se discute el origen de la Ti-clinohumita.

Palabras clave: Ti-clinohumita; mármoles; skarn de Ciénaga; mineralogía; Macizo Sierra Nevada de Santa Marta.

Record

Manuscript received: 11/07/2013

Accepted for publication: 26/10/2014

INTRODUCTION

The humite-group minerals have a limited paragenesis and occurs in marbles and skarns generated by contact metamorphism. However, they may also form in rocks affected by metasomatic processes linked to the regional metamorphism or hydrothermal alteration. Clinohumite is an uncommon member of the humite group, a magnesium silicate with the chemical formula $(Mg,Fe)_9(SiO_4)_4(F,OH)_2$, which is essentially a hydrated olivine. It is a mineral found as small grains in marbles of contact metamorphic environments. It is sporadically mined gem-quality in the Pamir Mountains of Tajikistan, and the Taymyr region of northern Siberia. Other (non-gem quality) occurrences of clinohumite include several localities around the world, such as Buell Park and San Juan County (USA), Ambasamudram (Southern India), Jacupiranga Complex (Brazil), Isua supracrustal belt (West Greenland), Malenco (Italy), Almiraz Massif (Spain), northeastern Jiangsu, Su-Lu, Dabie Mountains (China), Western Liguria (Italy), Kokchetav Massif (Kazakhstan). Ti-poor and F-rich clinohumite have been reported in metamorphic and metasomatic carbonate-rocks adjacent to acid plutonic intrusions (Fujino and Takeuchi, 1978; Satish-Kumar and Niim, 1998). Contrary to this, Ti-rich and F-poor clinohumite has been reported most frequently in ultramafic rocks. It was described from ultramafic xenoliths in carbonatites (Gaspar, 1992) and kimberlites (McGetehin et al., 1970; Aoki et al., 1976), found to be associated with antigorite in serpentinites (Trommsdorff and Evans, 1980; Sánchez-Vizcaino et al., 2005) and also occurs in metadunite (Dymek et al., 1988), in several garnet peridotites from ultrahigh-pressure (UHP) metamorphic terranes (Yang et al., 1993; Okay, 1994; Zhang et al., 1995; Yang, 2003), in metagabbros (Scambelluri and Rampone, 1999) and in a garnet-rich rock from the Kokchetav UHP metamorphic terrane of northern Kazakhstan (Muko et al., 2001). In this study, we report and discuss data concerning this unusual humite-group mineral at the Ciénaga skarn, Sierra Nevada de Santa Marta (SNSM) massif, with the aim of characterize its occurrence and determine its petrologic significance.

Geological setting

The SNSM massif constitutes an isolated triangular-shaped range in the northern Caribbean region of Colombia and represents an uplifted area located along the southern Caribbean plate boundary (Figure 1), a margin owing its character to the oblique convergence and right-lateral shearing between the Caribbean plate and northwestern South America (Moreno-Sánchez and Pardo-Trujillo, 2003). Its tectonic limits are the right-lateral Oca fault, the left-lateral Santa Marta-Bucaramanga fault, the Cerrejón thrust, and the Romeral suture. This massif is mainly composed of crystalline rocks and can be divided into three different belts (geotectonic provinces) with a well-defined outboard younging pattern from east to west: Sierra Nevada, Sevilla and Santa Marta. The southeastern and oldest belt (Sierra Nevada Province) includes ca. 1.0-1.2 Ga high grade metamorphic rocks represented by granulites, gneisses and amphibolites related to the Grenvillian orogenic event (Restrepo-Pace et al., 1997; Ordoñez et al., 2002; Cordani et al. 2005). Jurassic plutons and volcanites intrude and cover these metamorphic rocks and minor Carboniferous and Late Mesozoic sedimentary sequences rest in unconformity towards the southeast flank (Rabe, 1977). The intermediate belt (Sevilla province) represents a polymetamorphic complex that includes gneisses and schists of Paleozoic age with Permian mylonitic granitoids (Tschanz et al., 1969; Cardona et al., 2006; Cardona et al., 2010). The northwestern and youngest belt (Santa Marta province) comprises two metamorphic belts; an inner belt composed of imbricated metamorphic rocks (greenschists and amphibolites) of Cretaceous age and an outer belt formed of Mesozoic amphibolites, greenschists and phyllites separated from the lower to middle Cenozoic Santa Marta Batholith (Doolan, 1970; MacDonald et al., 1971; Tschanz et al., 1974). The Cesar-Ranchería basin is exposed on the southeastern flank of the Santa Marta Massif and represents a sedimentary record that evolved from Cretaceous passive margin to Maastrichtian-Paleogene orogenic deposits that are linked to an accretionary and subduction related event of the Caribbean

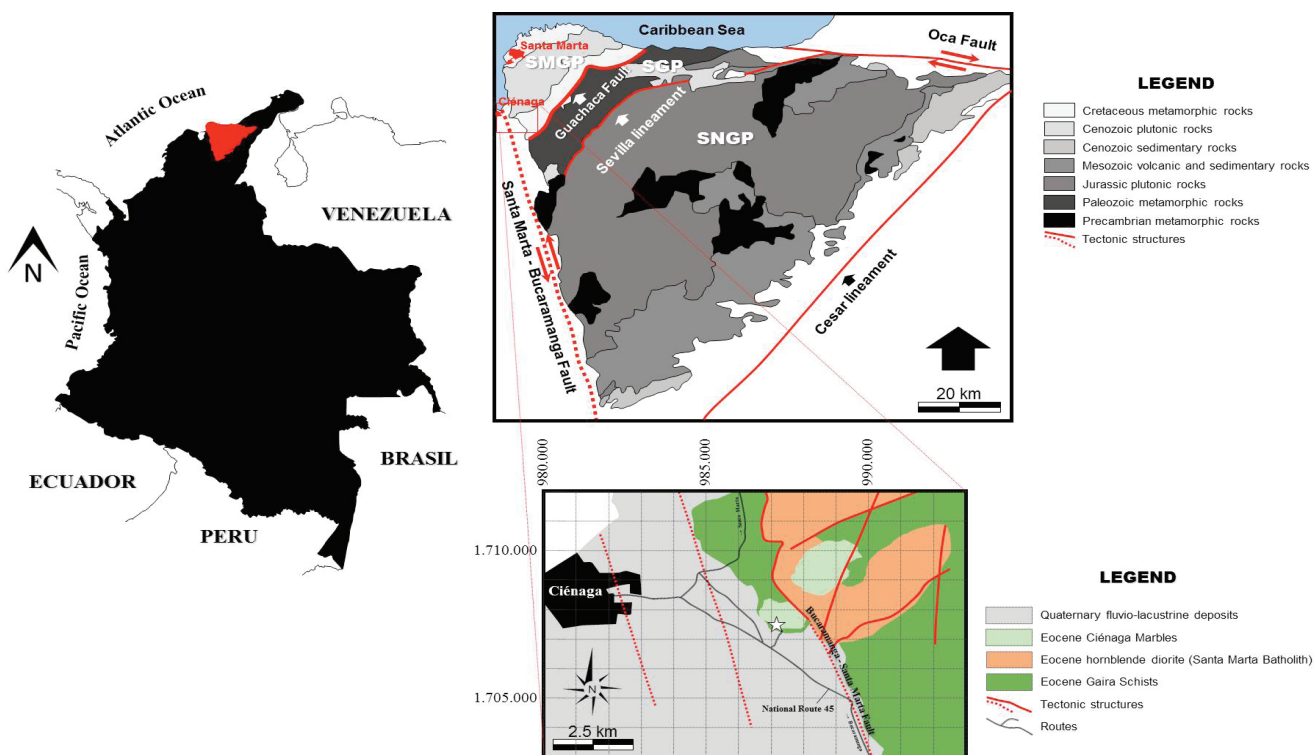


Figure 1. Geologic sketch map of the Ciénaga Marbles (modified after Hernández and Maldonado, 1999), showing its distribution in the study area. The open star indicates the location of the Ti-clinohumite marble. SMGP, Santa Marta Geotectonic Province; SGP, Sevilla Geotectonic Province; SNGP, Sierra Nevada Geotectonic Province.

plate (Bayona et al., 2007). The geological unit of interest in this study corresponds to the Ciénaga Marbles, initially reported by Tschanz et al. (1969) to describe marbles and limestones outcropping in two small bodies located eastward of the Ciénaga town, lying in apparent discordance with the lower unit of the Gaira Schists and cut by the Santa Marta Batholith. Interbedded marble layers in schists have also been reported by Tschanz et al. (1970). Hernández (2003) assigned a geological age of 50.7 ± 2.1 Ma to the Ciénaga Marbles on the basis of their stratigraphic position within the Gaira Schists. The Ciénaga Marbles include carbonates and siliceous carbonates affected by regional metamorphism. In the Ciénaga Marbles, the typical skarn mineral association has been recognized by Castellanos et al. (2013) and they will be the goal of the present contribution.

Field sampling and analytical methods

Ti-clinohumite-bearing marble was collected from a marble quarry of the Ciénaga skarn. The preparation of polished sections and thin sections for microscopic analysis performed according to the standard method in the Sample Preparation Laboratory of the Geology Program at the Universidad de Pamplona (Colombia), and the mineralogical and petrographic analysis of samples performed at the Laboratory of Microscopy of the Research Group in Basic and Applied Geology of the School of Geology at the Universidad Industrial de Santander (Colombia), using a trinocular NIKON (Labophot2-POL) transmitted light microscope to establish the modal percentage of mineral constituents and mineral assemblages, with emphasis on textural relationships between mineral phases. Additional analysis was developed at the laboratory of microscopy of the, using a trinocular OLYMPUS (BX-51) transmitted light microscope in order to take microphotographs using a NIS-Elements Br Microscope Imaging Software of the Geology Program at the Universidad de Pamplona (Colombia). Mineral abbreviations are after Kretz (1983), Siivola and Schmid (2007) and Whitney and Evans (2010). Polished thin sections were coated by carbon evaporation technique using a carbon cord quorum Q150R ES system before SEM analysis. SEM-BSE/EDS imaging and analysis were carried out by field emission gun environmental scanning electron microscopy (FEI Quanta 650 FEG SEM) of the Laboratory of Microscopy at the Universidad Industrial de Santander, Guatiguará Technological Park (Colombia) to examine the mineral phases, textures and cross-cutting relationships in the Ti-clinohumite marble, under the following analytical conditions: magnification = 150-600x, WD = 9.4-10.6 mm, HV = 20 kV, signal = Z Cont, detector = BSED. 17 seconds counting for points analyzed with 12.000 counts. Semiquantitative EDS analysis (standardless quantitative analysis) which does not require calibration standards was performed. The typical detection limit for EDS is 0.1wt%. Quantification was performed with type ZAF matrix correction.

Field occurrence

The field occurrence of marbles in the Ciénaga skarn reveals that they show a variable morphology (with sharp contacts) and thickness with a transition into carbonate-silicate rocks, which consecutively pass into calc-silicate and carbonate-bearing silicate rocks. When carbonate tends to disappear, they pass into granodiorites. The marble horizon in which Ti-clinohumite occurs (Figure 2) forms part of the Ciénaga Marbles geological unit. Marbles are white and sometimes pale green, gray or yellow in color, and medium- to coarse-grained, and their thickness ranges from 7.5 to 10 cm up to 1.5 m in thickness (Figures 2a-c). They show banding foliation and they are characterized by the alternation of carbonate-rich zones (from 1 to 3.5 mm up to 1 cm in thickness) with different mineral assemblages, which display sharp contacts and discontinuous bands of lenticular geometry within the metamorphic sequence. Marbles are frequently arranged in bands or patches with different colors being some shade of red, pink, yellow or green, which are caused by the presence of impurities, such as clay minerals or iron oxides, which were originally present as grains or layers in their protoliths, and add to their beauty when they are cut and polished. These marbles contain different proportion of calcite and dolomite and were intensely replaced by skarn mineral association. Ti-Clinohumite-bearing

marble occurs as reddish-brown tiny bands interbedded in white marble parallel to the regional schistosity (Figures 2d-f). It is a white to reddish-brown coarse-grained rock composed of calcite, dolomite, Ti-clinohumite, forsterite, diopside, accessory clinocllore, muscovite, fluorapatite and shining flakes of graphite. Serpentine is the main alteration product. Ti-clinohumite-bearing folded bands were also observed (Figures 2d and 2e). These marbles have been locally replaced by abundant skarn mineral association near the contact with orthoamphibolites, which are crosscut by pegmatitic veins. Contacts between marbles and orthoamphibolites are subparallel to the main mesoscopic foliation, although the development of the skarn mineral association is not always clearly related to these contacts.

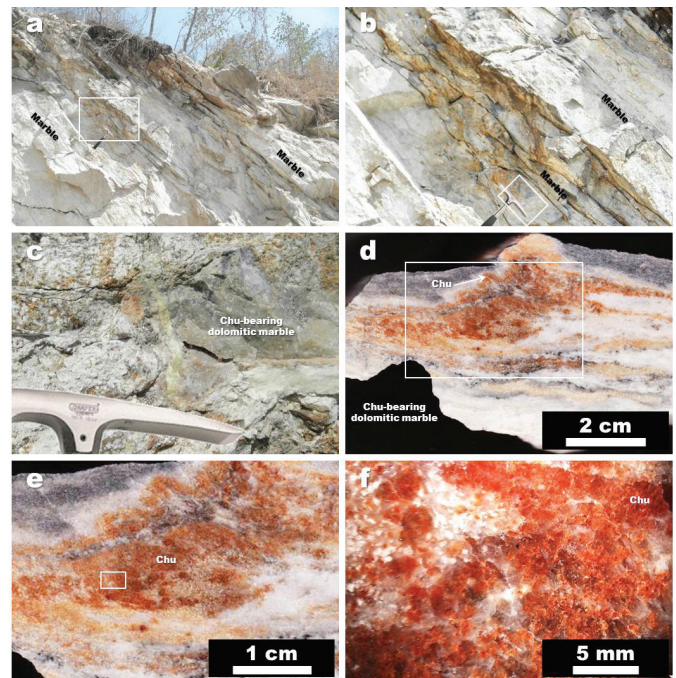


Figure 2. Field (a-c) and hand-specimen (d-f) photographs of Ti-clinohumite marble in the Ciénaga skarn, Sierra Nevada de Santa Marta Massif.

Petrography

The Ciénaga Marbles are mainly calcite-rich marbles with bands parallel to the regional trend (N35-45oNE and 20-45oSE) showing different mineral assemblages. These are composed of calcite bands in a proportion of more than half of the mode and the variations in the mineral assemblages are defined by the Mg-rich phases. Castellanos and co-workers (personal communication) described in detail the characteristic mineral assemblages from reaction zones recognized in marbles, which include calcite + graphite ± quartz; calcite + diopside ± tremolite ± epidote-group minerals ± muscovite; calcite + wollastonite + quartz + garnet + diopside; calcite + dolomite + Ti-clinohumite + diopside + forsterite + clinocllore ± graphite; calcite + forsterite + tremolite; dolomite + calcite + clinocllore. Accessory minerals are fluorapatite, muscovite, rutile and titanite.

The rock of interest in this study corresponds to a Ti-clinohumite marble, which display a granoblastic texture. It is composed of several reaction zones (Figure 3), which are described as follows: (1) grey color reaction zone (2-8.5 mm in thickness) consisting of calcite + dolomite + graphite; (2) light grey color reaction zone (1-3.5 mm in thickness) consisting of diopside + calcite ± tremolite; (3) brown reddish color reaction zone (1.5-20 mm in thickness) consisting of Ti-clinohumite + calcite + clinocllore ± muscovite ± fluorapatite ± graphite; (4) orange color reaction zone (2-6.5 mm in thickness) consisting of Ti-clinohumite + calcite + dolomite + clinocllore + rutile ± muscovite; (5) light yellow color reaction zone (2-5.5 mm in thickness) consisting of dolomite + calcite + forsterite (antigorite).

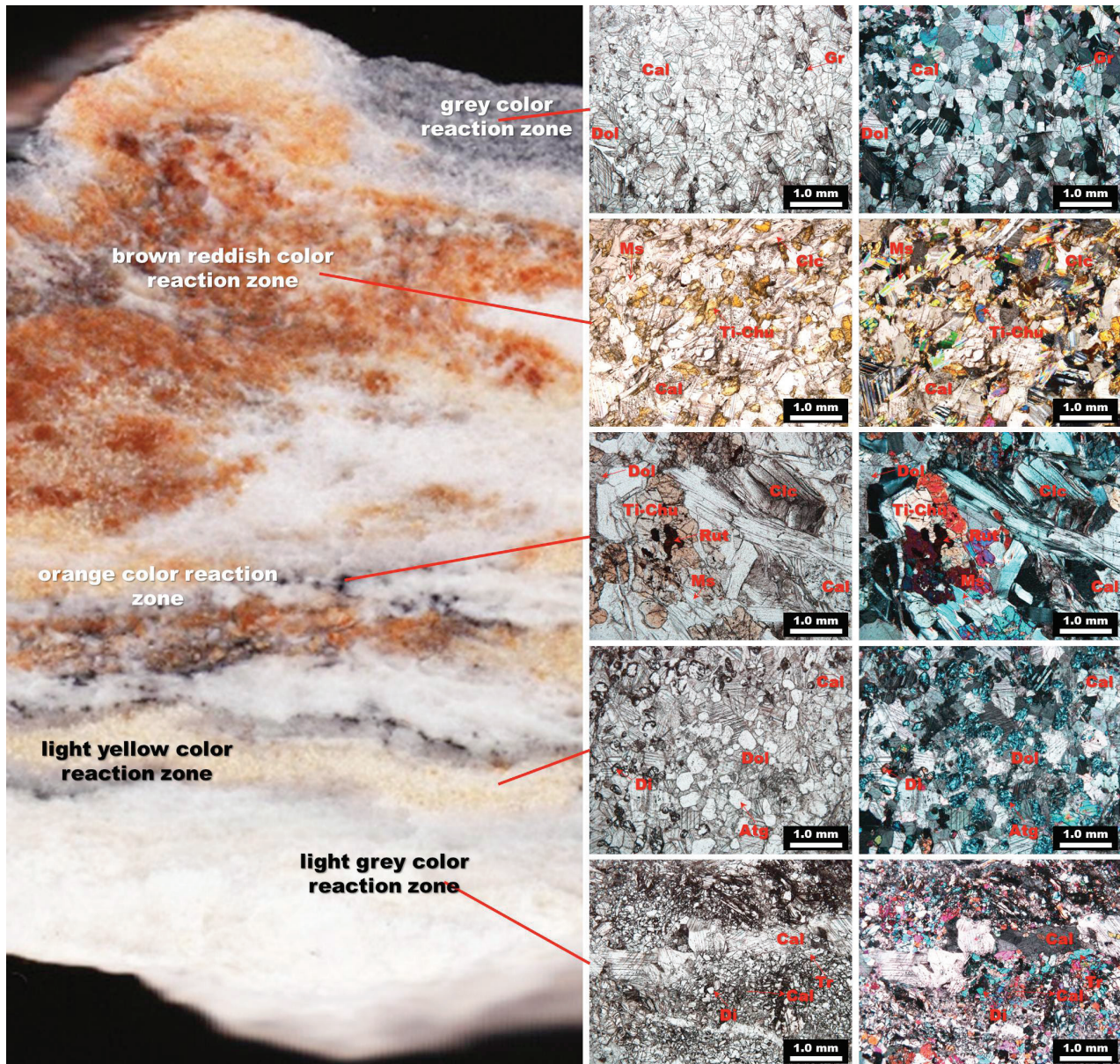


Figure 3. Left, a photograph of the polished section of the Ti-clinohumite marble, showing different reaction zones. Right, photomicrographs in Plane Polarized Light (PPL) and Cross Polarized Light (XPL) of the reaction zones. Dol, dolomite; Cal, calcite; Di, diopside; Clc, clinocllore; Ti-Chu, Ti-clinohumite; Tr, tremolite; Atg, antigorite; Ms, muscovite; Rut, rutile; Gr, graphite.

Ti-clinohumite associated mineral phases

Calcite (80-95%) occurs in two generations. The first one occurs as medium-grained individuals with heteroblastic to subidioblastic shape (Figure 4), showing characteristic rhombohedral cleavage and polysynthetic twinning. It occurs through most of the sample as an intergrowth with dolomite (15-75%) rhomb sections (Figures 4a-b, 8d-f). Domains with Ti-clinohumite (Figures 5, 6, 7, 8a-b) and fluorapatite (Figures 7, 8a, g) are cross-cut by veinlets of very fine- to medium-grained xenoblasts of calcite. Diopside (5-20%) occurs in the sample as a very fine-grained granoblastic intergrowth with calcite (Figures 4c-d). It shows a heteroblastic to subidioblastic contours, high relief and first and second order interference colors (from red to violet and blue). Clinocllore (5-10%) is colorless to pale green and can be recognized by its flaky to fibrous character, excellent one direction cleavage and very low birefringence (Figures 4e-f, 7, 8a-b).

Tremolite (1-5%) occurs as colorless crystals of moderate to high relief and first to second order interference colors, which are in contact with calcite (Figures 4c-d). Graphite (1-5%) occurs as scarce tiny flakes (Figure 7). Forsterite (<1%) is characterized by cracked round grains, which show up in bright interference colors (Figure 7). It can be replaced by antigorite (Figure 8h). Fluorapatite (<1%) occurs as small grains (up to 250 μm) are usually idioblastic and closely associated with Ti-clinohumite grains and clinocllore (Figures 7, 8a). Rutile (<1%) displays its typical brown reddish color (Figures 4e-f, 5c-d). Titanite (1%) use to develop a reaction rim around rutile (Figures 5c-d). Muscovite (<1%) is colorless and can be recognized by its flaky character and excellent one direction cleavage (Figure 6). Antigorite (0-10%) appears as a fibrous product of alteration along irregular fractures of forsterite (Figure 7) and pseudomorphic replacement after diopside grains (Figures 5e-f) grains.

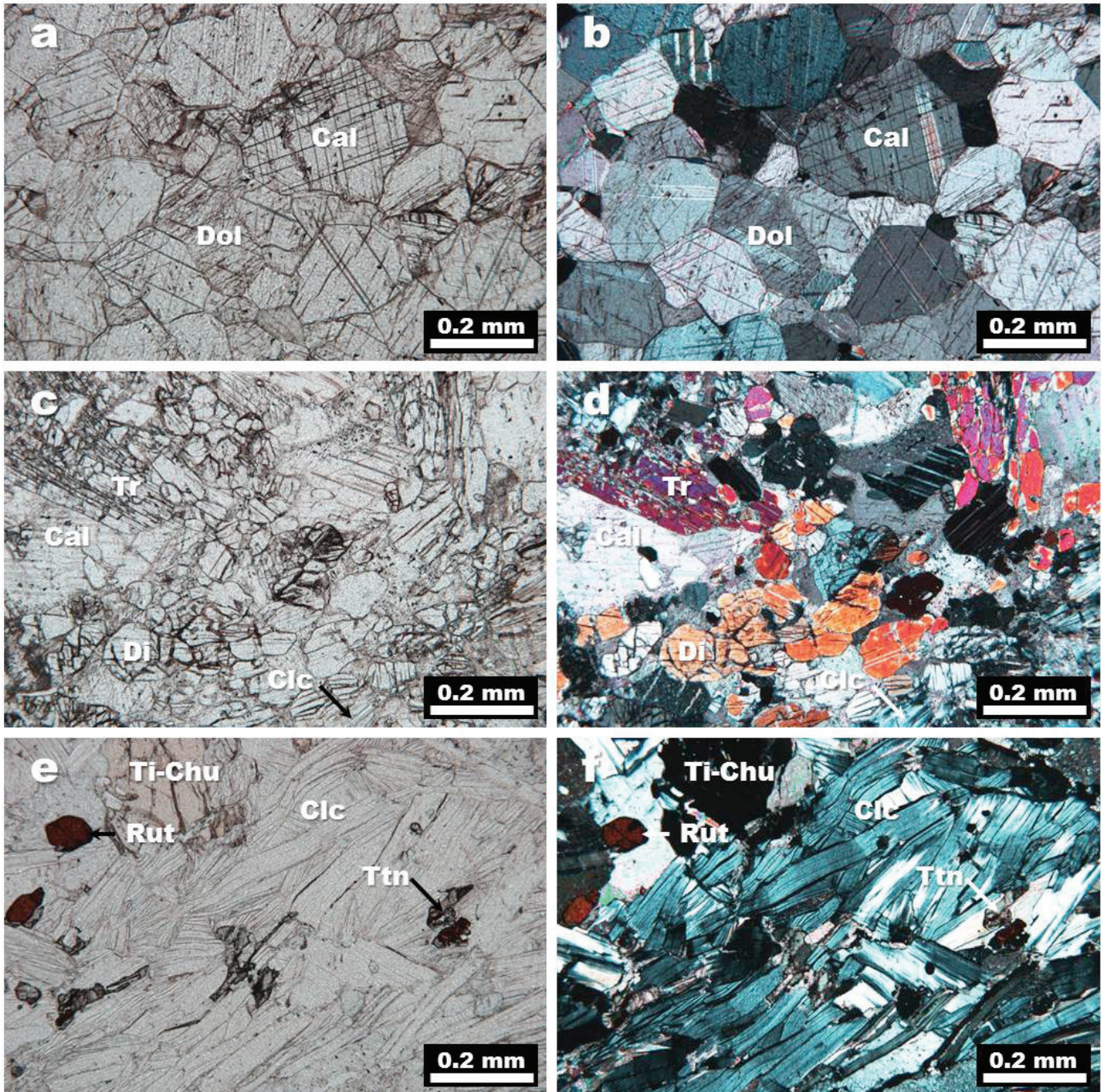


Figure 4. Photomicrographs showing the representative textural relationship between minerals in the Ti-clinohumite-bearing marbles in (a), (c), (e) PPL and (b), (d), (f) XPL. Dol, dolomite; Cal, calcite; Di, diopside; Clc, clinocllore; Ti-Chu, Ti-clinohumite; Tr, tremolite; Rut, rutile; Ttn, titanite.

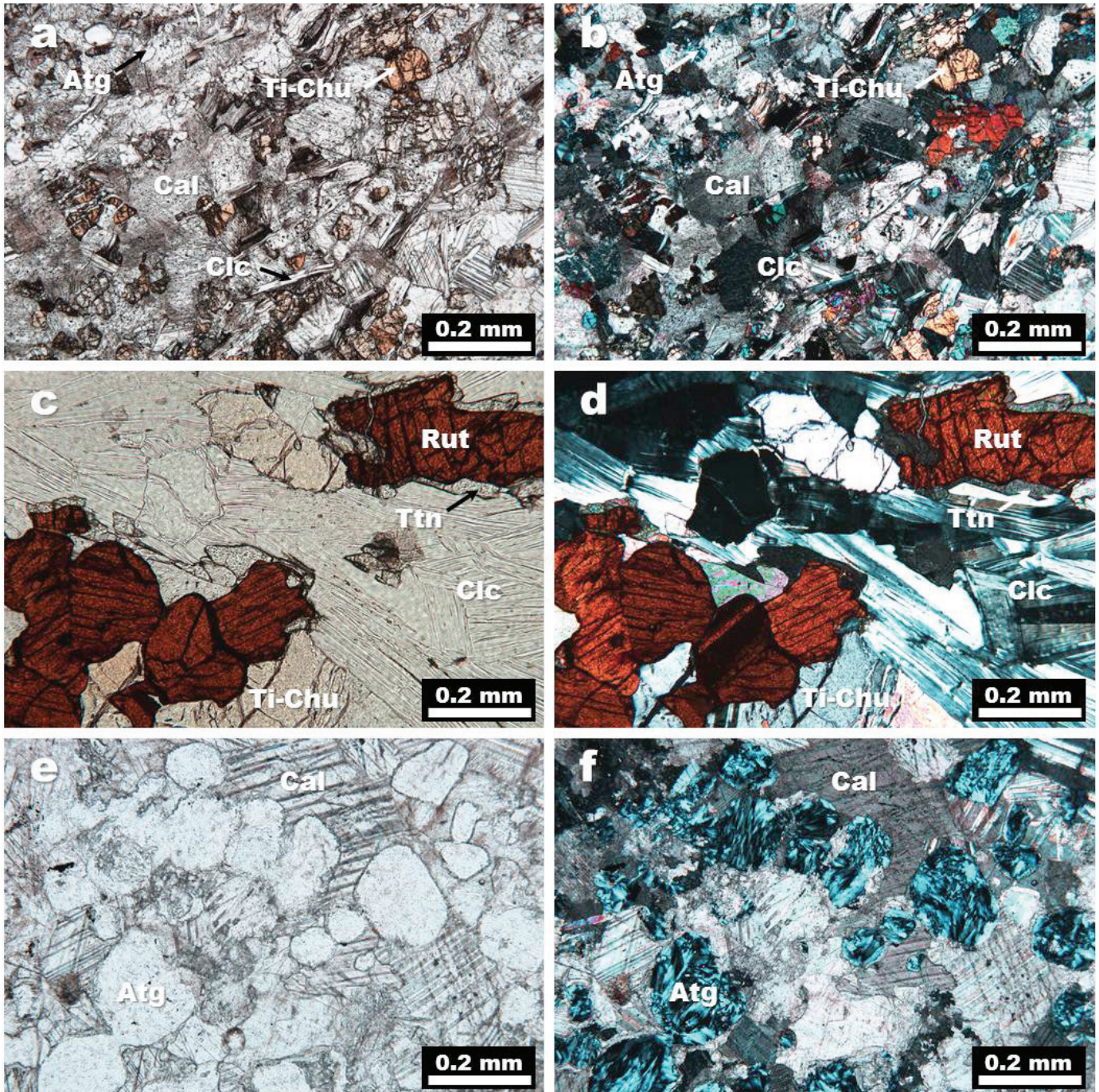


Figure 5. Photomicrographs showing the representative textural relationship between minerals in the Ti-clinohumite-bearing marbles in (a), (c), (e) PPL and (b), (d), (f) XPL. Cal, calcite; Ti-Chu, Ti-clinohumite; Clc, clinochlore; Rut, rutile; Ttn, titanite; Atg, antigorite.

Ti-clinohumite

Alternating calcite-rich with dolomite and dolomite-rich with calcite bands are observed in the analyzed sample. However, domains rich in Ti-clinohumite are mainly related to the calcite-rich with dolomite bands as shown in Figure 7. The Ti-clinohumite-bearing domains show a granoblastic polygonal texture (Figures 5a-b, 8c-d, f), with the mineral assemblage: calcite + dolomite + Ti-clinohumite + forsterite + diopside + clinochlore + fluorapatite ± rutile ± muscovite ± graphite, where the small grains of Ti-clinohumite can be preserved within large calcite grains (Figures 7, 8i). Ti-clinohumite (10-55%) occurs predominantly as xenoblasts (up to 2 mm in diameter) in granoblastic

calcite-rich bands. These xenoblasts usually show patchy pleochroism varying within individual grains due to compositional variations and irregular zoning patterns and also can develop twinned grains (Figure 6). Ti-clinohumite grains can also occur spatially related with clinochlore and muscovite (Figure 6). Very fine-grained and rounded pseudomorphs of antigorite after diopside disseminated around calcite are illustrated in Figures 5e-f. Rough intergrowths of Ti-clinohumite with forsterite are very common (Figures 8f, i). Ti-clinohumite occasionally contains scarce inclusions of clinochlore and rutile. Titanite rims around rutile are commonly observed near Ti-clinohumite.

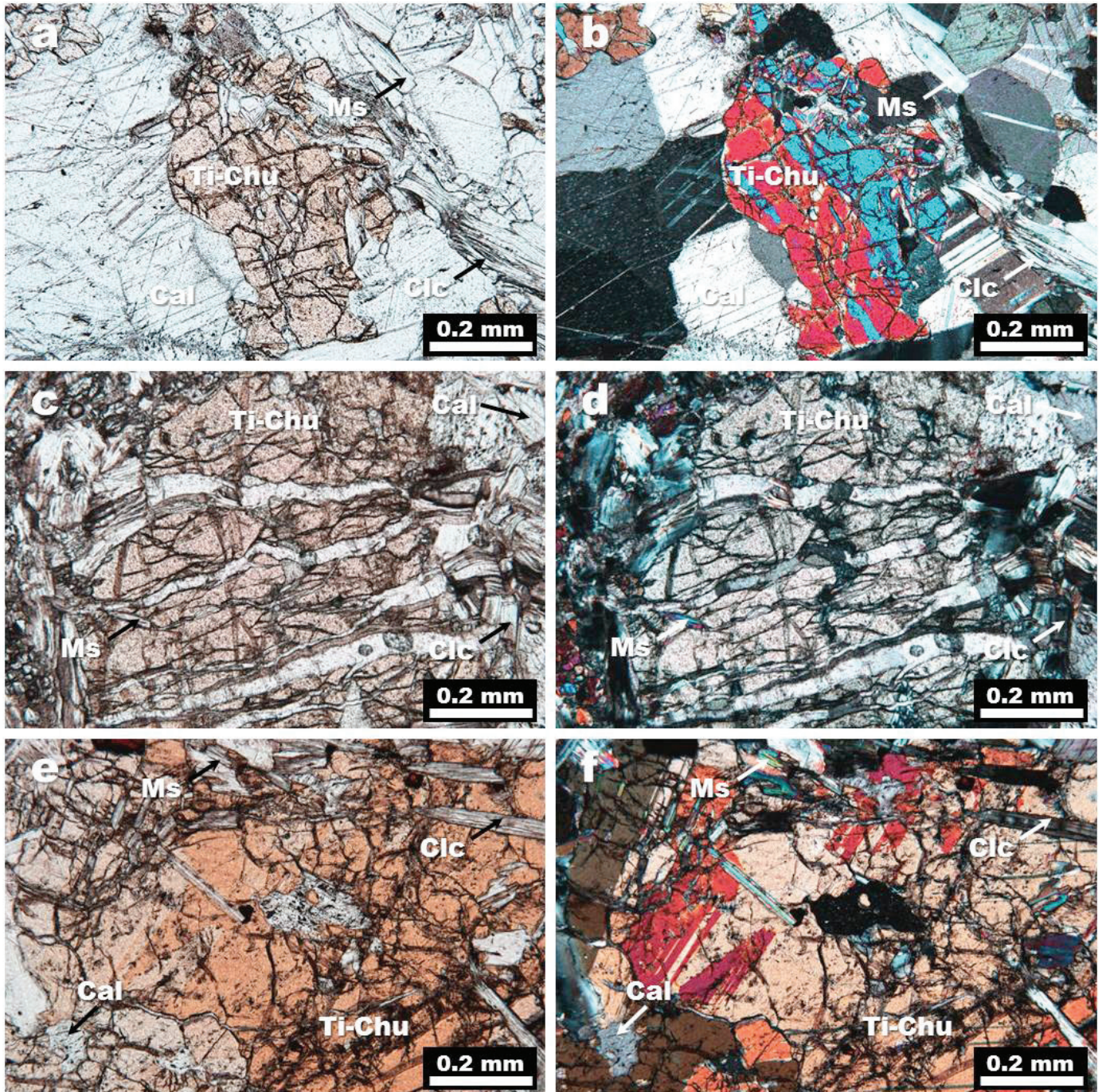


Figure 6. Photomicrographs display the occurrence of the Ti-clinohumite and associated mineral phases. (a), (c), (e) PPL and (b), (d), (f) XPL. Cal, calcite; Di, diopside; Chu, Ti-clinohumite; Ms, muscovite; Clc, clinocllore.

An overview high resolution image mosaic of the Ti-clinohumite bearing marble is presented in Figure 7. An irregular crack cross cut at high angle the metamorphic foliation of the rock. Note the high-

density fluorapatite (to the right) from the backscatter electron image contrast. Figure 8 shows several examples of the textural relationships between Ti-clinohumite and associated mineral phases.

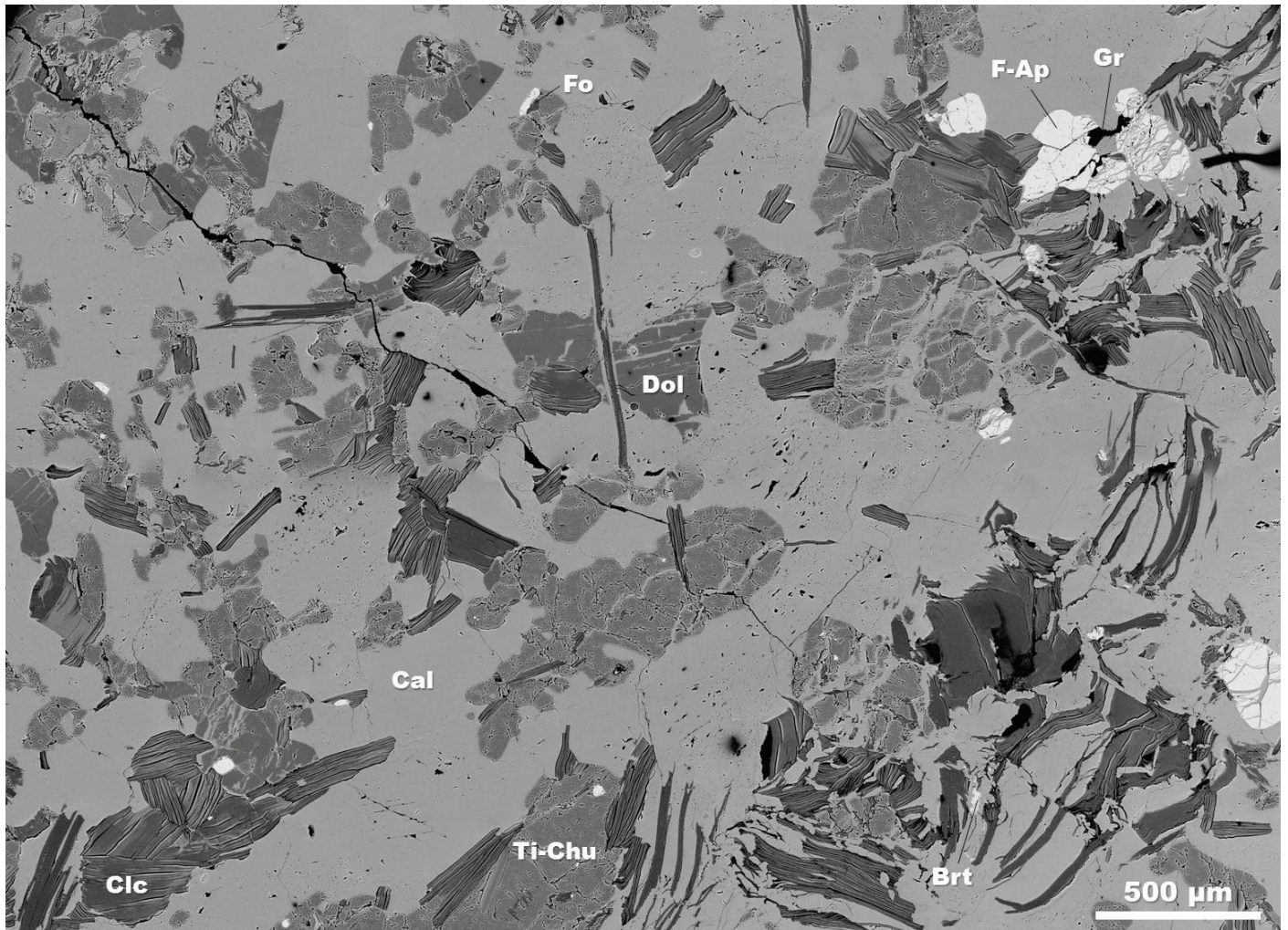


Figure 7. High resolution backscattered electron image mosaic of the Ti-clinohumite bearing domain in calcite-rich marble. An irregular crack cross cut at high angle the metamorphic foliation of the rock. Note the high-density fluorapatite (top-right corner of the image). Fo, forsterite; Cal, calcite; Dol, dolomite; Ti-Chu, Ti-clinohumite; Clc, clinochlore; F-Ap, fluorapatite; Gr, graphite; Brt, barite.

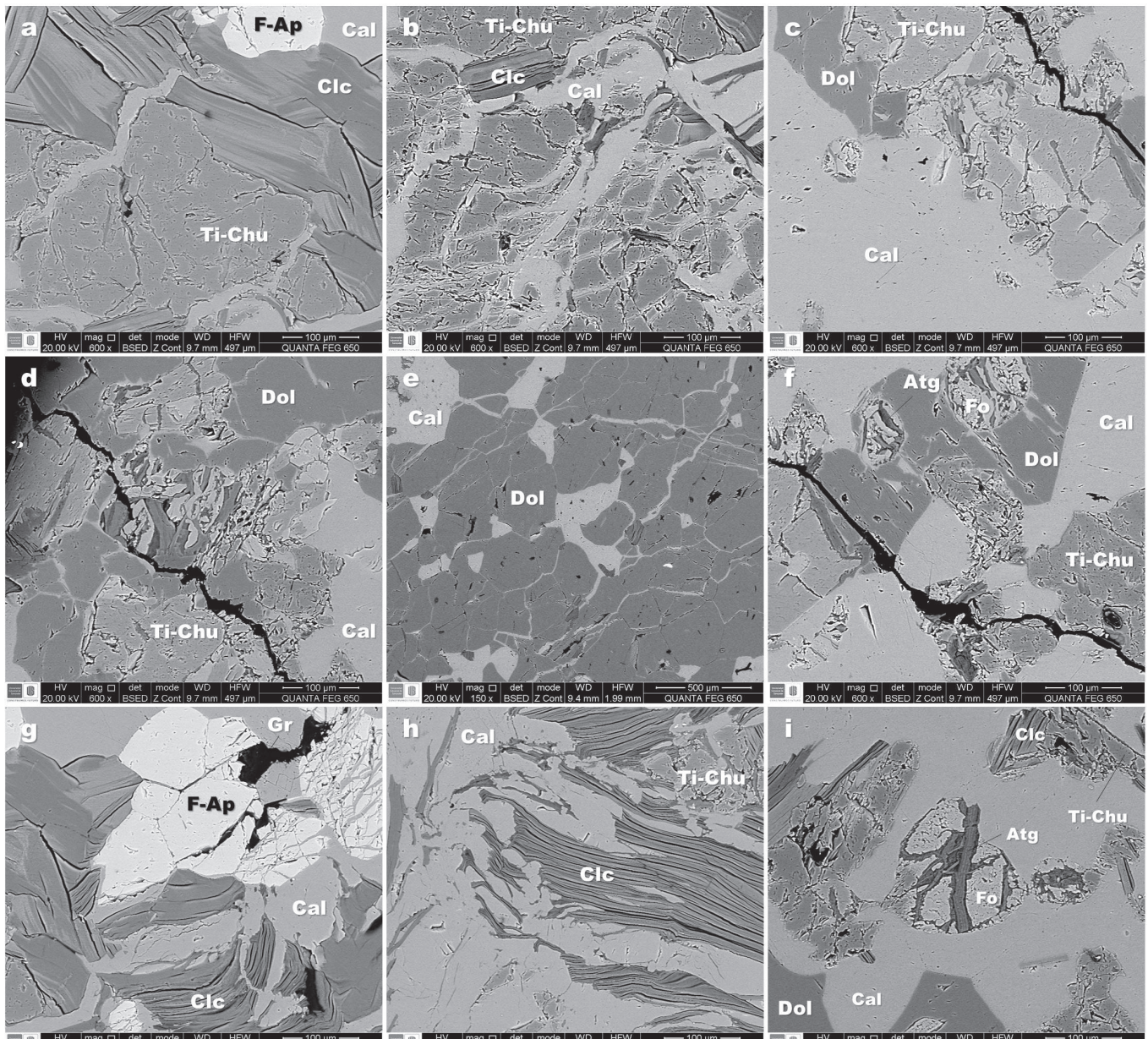


Figure 8. Backscattered electron images of the textural relationships between Ti-clinohumite and associated mineral phases. Cal, calcite; Dol, dolomite; Ti-Chu, Ti-clinohumite; Fo, forsterite; Atg, antigorite; Clc, clinocllore; F-Ap, fluorapatite; Gr, graphite. (a) Relationship between Ti-clinohumite and clinocllore, calcite and fluorapatite; observe secondary veins of calcite cross cutting minerals and non-optical continuity of gray color in clinocllore. (b) Numerous secondary veins of calcite cross cutting Ti-clinohumite, which is associated with calcite and clinocllore. (c) Association dolomite + calcite, which are in contact with Ti-clinohumite; observe secondary veins of calcite cross cutting minerals and non-optical continuity of gray color in clinocllore. (d) The occurrence of Ti-clinohumite along with dolomite + calcite. (e) Dolomite predominance with scarce calcite, which occurs as a matrix phases or as secondary veins cross cutting dolomite. (f) Association calcite + dolomite + Ti-clinohumite + forsterite (replaced by antigorite). (g) Occurrence of fluorapatite along with calcite and clinocllore; numerous veins of calcite cross cut fluorapatite; with graphite filling microfractures. (h) Association clinocllore, calcite and highly corroded Ti-clinohumite. (i) Replacement of forsterite by antigorite; notice also the presence of Ti-clinohumite, dolomite, calcite and clinocllore.

The SEM image in Figure 9 shows the textural relationships between Ti-clinohumite and its associated mineral phases. The semi-quantitative Energy Dispersive Spectroscopy (EDS) analyses at different points marked with stars allowed identifying the particular elements and their relative proportions in the mineral phases analyzed in the Ti-clinohumite-bearing domains of the calcite-rich marbles. The EDS analysis revealed that mineral phases in the analyzed sample correspond to: calcite (1) has 79.95 wt% CaO and 15.65 wt% CO₂, with minor MgO (4.40 wt%); dolomite (2) with 50.10 wt% CaO, 34.59 wt% MgO and 15.31 wt% CO₂. Forsterite (3) is characterized by high contents of MgO (50.15 wt%) and SiO₂ (47.47 wt%), with minor FeO (2.38 wt%). Antigorite

(4) reveals the presence of 62.91 wt% SiO₂, 24.72 wt% MgO, and minor Fe₂O₃ (2.59 wt%) and CaO (0.93 wt%). Diopside (5) indicates the presence of CaO (19.48 wt%), MgO (18.91 wt%) and SiO₂ (61.61 wt%). Clinocllore (6) reveals 31.18 wt% MgO, 13.71 wt% Al₂O₃, 1.07 wt% FeO, 53.69 wt% SiO₂. Fluorapatite (7) shows the presence of CaO (53.87 wt%), P₂O₅ (42.79 wt%) and F (2.87 wt%). Ti-clinohumite (8) reveals that it consists of MgO (50.87 wt%) and SiO₂ (44.01 wt%), with minor FeO (2.12 wt%). It can be considered as a Ti-clinohumite taking into account the incorporation of up to 2.57 wt% of Ti in its mineral structure. EDS spectra are in agreement with literature data (<http://www.sfu.ca/~marshall/sem/mineral.htm>).

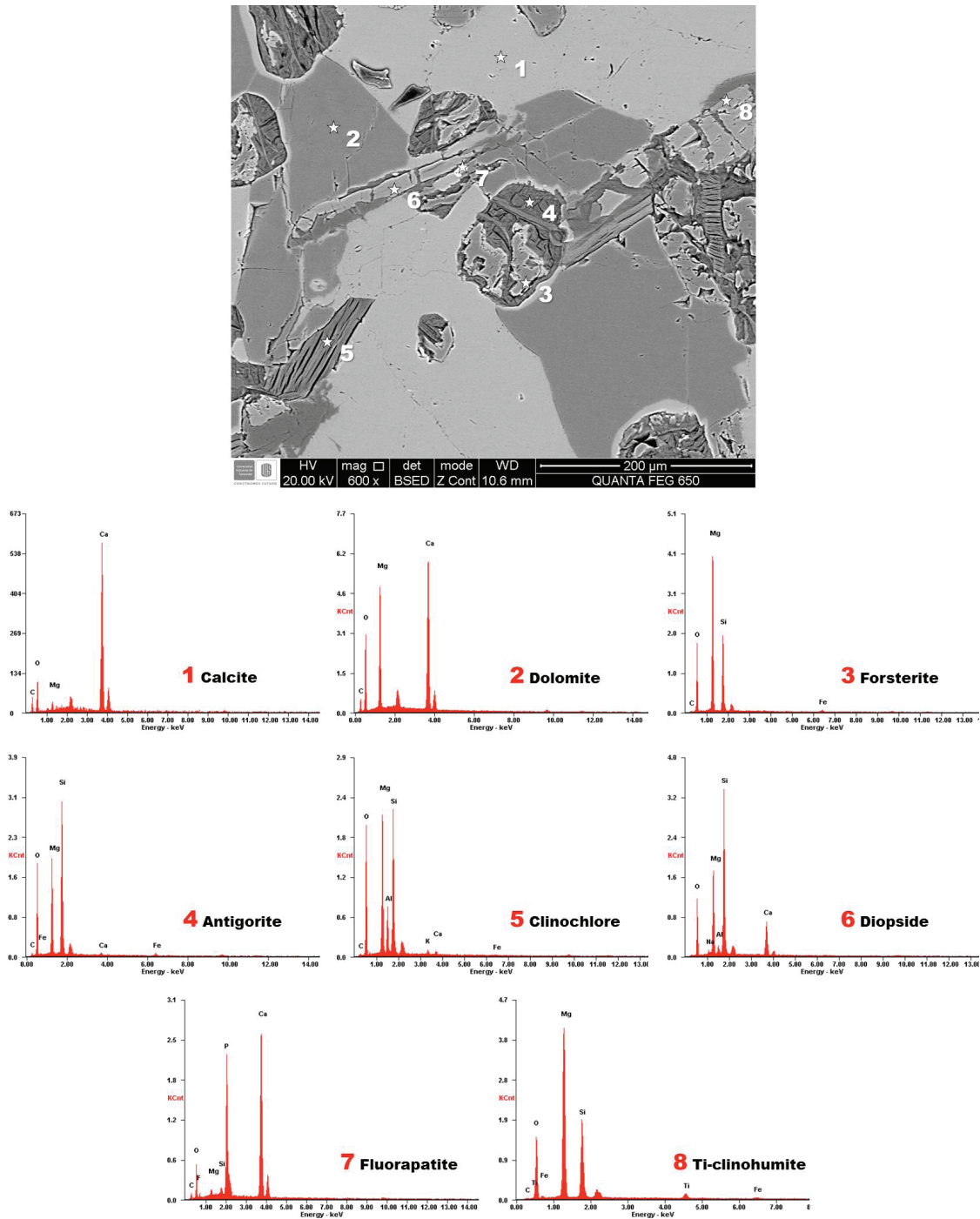


Figure 9. SEM image and EDS spectra of the analyzed mineral phases (marked with stars on the image) of Ti-clinohumite-bearing domains in magnesium calcite-rich marbles. The appearance of C element is attributed to the carbon coating on the sample before SEM analysis.

Figure 10 shows the elemental mapping of Ti-clinohumite and associated mineral phases, which however will only give a qualitative illustration of the distribution of elements. Ti and Fe show a similar pattern of distribution with low concentration of these elements in the Ti-clinohumite, except by the occurrence of rutile that displays a high content of Ti. The content of Mn is regularly distributed in the

sample. Note also a similar pattern of distribution for Mg and Si with a high concentration of these elements in the Ti-clinohumite. However, the highest contents of Mg reveal the occurrence of Mg-rich chlorite (clinocllore), which occurs both as inclusions in Ti-clinohumite and as a matrix phase. The distribution of Al also reveals not only its low content in Ti-clinohumite but also the high content in clinocllore.

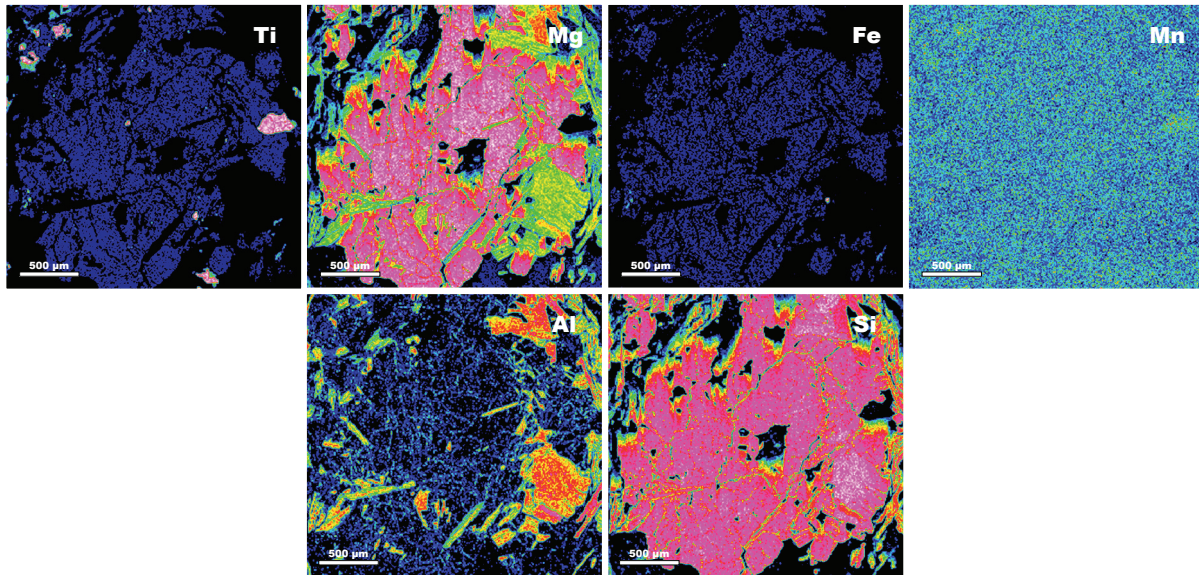


Figure 10. Compositional maps of Ti-clinohumite and associated mineral phases for Ti, Mg, Fe and Mn (above), and Al and Si (below). Light colors show areas of high concentration while dark colors represent areas of low concentration (black is very low concentration).

Figure 11 illustrates a binary diagram of $MgO/(MgO+FeO+MnO)$ vs. TiO_2 for the compositions of Ti-clinohumite from several geological environments. According to Gaspar (1992), this diagram takes into account the two most effective substitutions in Ti-clinohumite: Mg by Fe (and Mn) and $Mg(FOH)_2$ by TiO_2 . Even the analyzed Ti-clinohumite from

the Ciénaga Marbles does not match with any of the compositional fields defined by Gaspar (1992), it represents not only a Ti-clinohumite almost pure in Mg but also may be some of the most Mg-rich and TiO_2 -rich varieties around the world for skarn environments.

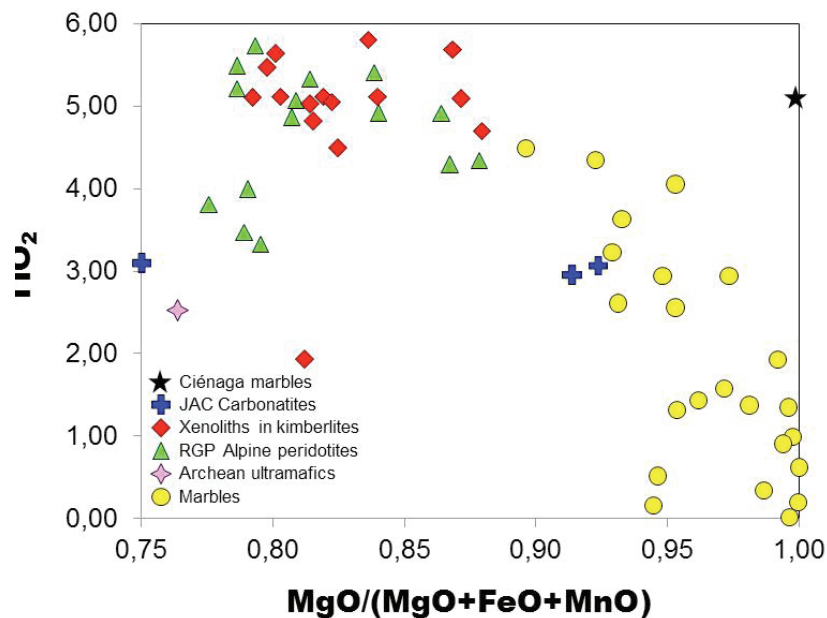


Figure 11. $MgO/(MgO+FeO+MnO)$ vs. TiO_2 diagram, showing the compositions of the Ti-clinohumite from several geological environments, including the analyzed sample in this study indicated in black star (adapted and modified after Gaspar, 1992).

Discussion on the origin of Ti-clinohumite and its petrologic significance

The Ciénaga Marbles were affected by emplacement of granodioritic rocks belonging to the Santa Martha Batholith, developing a skarn-type mineralogy as suggested by Castellanos and co-workers (personal communication), which gives rise to thin reaction zones. However, we suggest that the skarn-type mineralogy hosted in this metamorphic unit should be related both magmatic and postmagmatic stages of the Santa Martha Batholith, and is the result of a very complex skarn-type mineralogy zonation (Castellanos and co-workers, personal communication).

Calcareous rocks (marbles, metacarbonates and calc-silicate rocks) represent only a relatively small fraction of the crust but their metamorphism is important because it can reveal significant information about the composition of the metamorphic fluid phase as well as P-T conditions (Spear, 1993). The regional fluid flow transporting volatiles including H₂O and CO₂ is an integral part of prograde regional metamorphism (Ague, 2003). According to Connolly and Trommsdorff (1991), isothermal or isobaric phase diagram sections as a function of the fluid composition are widely used for interpreting the genetic history of these rocks, although this approach has the following disadvantages: (1) the influence of key metamorphic variables such as P and T are obscured, and (2) the diagrams are inappropriate for systems that are not fluid-saturated. These problems are avoided by constructing phase-diagram projections in which the volatile composition of the system is projected onto a PT coordinate frame, i.e., a petrogenetic grid (Connolly and Trommsdorff, 1991). Mineral reactions in calcareous rocks can be modeled in the system CaO-MgO-SiO₂-H₂O-CO₂ (CMS-HC) However, other components (e.g., FeO, Al₂O₃, Na₂O, K₂O and TiO₂) are also present, playing a very important role in the stabilization of additional mineral phases such as micas, epidote-group minerals, garnet, feldspar, titanite, rutile. A petrogenetic grid for these rocks is most useful for the study of regional metamorphism and for systems in which fluid composition has not been externally controlled. Therefore, PT projection for this chemical system suggests that many assemblages in a mixed-volatile environment have stability fields that make them useful as P-T indicators (Connolly and Trommsdorff, 1991). One of the implicit assumptions to construct a T-XCO₂ reaction grid in this system is that there is a H₂O and CO₂ fluid present in all mineral assemblages, which are considered in "excess", consequently, only the remaining three "inert" components (CaO-MgO-SiO₂) are considered (Spear, 1993). Figure 12 illustrates a composition triangle for the system CMS-HC showing the plotting position of mineral phases considered in the Figure 13.

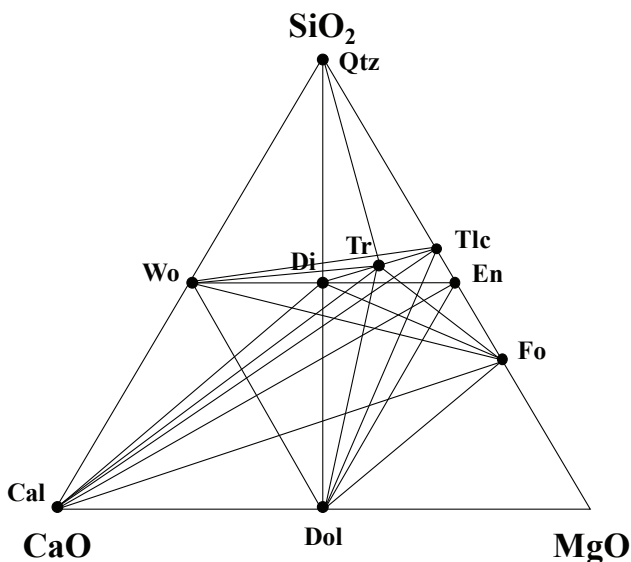


Figure 12. Composition triangle for the chemical system CMS-HC projected from H₂O and CO₂ showing the plotting position of mineral phases (modified after Spear, 1993).

According to Spear (1993), T-XCO₂ diagrams can be used to predict the sequence of metamorphic mineral assemblages and there are three mechanisms by which the calcareous rocks may evolve: (1) metamorphism at constant fluid composition, (2) metamorphism driven by infiltration, and (3) metamorphism in a closed system. The reactions encountered in progressive metamorphism generate H₂O and CO₂ that will tend to change the fluid composition, representing a problem for the first mechanism to evolve. This is why metamorphism at constant fluid composition, although easy to understand, is probably not representative of calcareous rocks of the Ciénaga Marbles. Instead the fluid infiltration process serves very well to explain driving devolatilization reactions in the Ciénaga Marbles. The sequence of mineral assemblages in the first two process is similar with the exception that diopside is not encountered up to ~ 570 oC (Spear, 1993), which can explain the occurrence of diopside associated with wollastonite in the Ciénaga Marbles. We suggest from field and petrologic evidence (occurrence of Ti-clinohumite and wollastonite, and the mineral assemblages calcite + quartz + diopside, calcite + diopside + wollastonite and quartz + diopside + wollastonite) that infiltration of H₂O-rich fluids within these marbles was probably driven by channeling along fractures and grain boundaries. Additional evidence includes the fact that Ti-clinohumite is not stable in pure H₂O-CO₂ fluids as suggested by Bucher and Frey (1994). On the other hand, calcareous rocks of the Ciénaga Marbles are surrounded by the pelitic Gaira Schists, which can drive decarbonization reactions as suggested by Spear (1993). This can be explained by a chemical reaction such as CaCO₃ (calcite) + SiO₂ (quartz) = CaSiO₃ (wollastonite) + CO₂ (e.g., Bucher and Frey, 1994; Ferry, 2000; Ferry et al., 2001), which can explain the formation of wollastonite in the Ciénaga Marbles by the interaction of marble with an H₂O-rich fluid as suggested by Bucher and Frey (1994). The H₂O released from the dehydration of pelitic schists probably infiltrated the calcareous rocks promoting decarbonization, which can explain the transformation of forsterite to Ti-clinohumite. We consider that infiltration may have been the dominant mechanism during contact metamorphism, with H₂O-rich fluids from the crystallization of a granodiorite intrusion penetrating calcareous rocks in the contact aureole giving rise to a skarn-type mineralogy and the formation of Ti-clinohumite, discussed in detail below. In the third mechanism, the fluid generated by devolatilization reactions remains in the rock and is mixed with the fluid that is already present, producing a fluid of a new composition (Spear, 1993). In this case, the evolution of the fluid is controlled by the mineral assemblage and most of the reaction progress will occur at isobaric invariant points. The process in which the fluid composition evolved in response to mineral reactions is called buffering.

T-XCO₂ diagrams are used to predict the sequence of metamorphic mineral assemblages that would be observed at constant fluid composition as shown in Figure 13. According to Winter (2001), there is a fluid-internal vs. external control. In the internal control (buffering assemblage), the mineral assemblage controls the composition of the H₂O-CO₂ fluid, representing a closed system; the buffer capacity is present until one of the phases completely consumed. In the external control, the extensive influx of fluids overrides buffer capacity mineral assemblages, representing an open system. However, taking into account that Ti-clinohumite is not stable in CO₂-rich fluids, it is better to consider that mineral assemblages with the presence of Ti-clinohumite reveal the influence of H₂O-rich fluids.

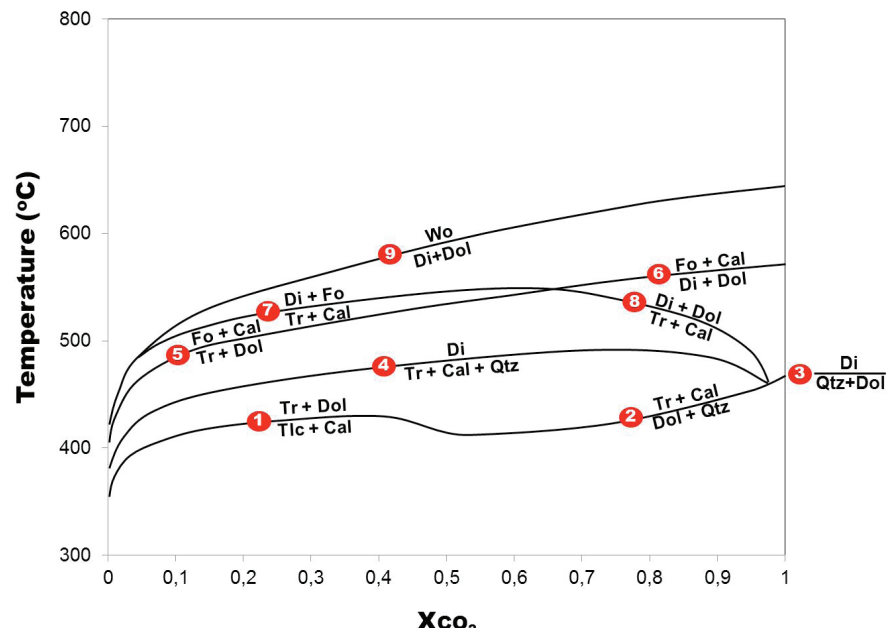


Figure 13. T-XCO₂ diagram for the system CMS-HC, showing boundary curves for carbonate-silicate reactions, according to Bucher and Frey (1994).

A textural intergrowth between calcite and dolomite can be interpreted as the result of exsolution of dolomite from calcite. Quartz and calcite, which are commonly found in contact in other samples from the study area, reveal sign of reaction to produce wollastonite. Therefore, since quartz and dolomite are considered to have been in disequilibrium everywhere and wollastonite was found in some of the samples of the Ciénaga Marbles, the area of interest in Figure 13 lies between the line defined by reactions 1-3 and the wollastonite curve (reaction 9) at high temperatures. However, this area is divided into two sub-areas, separated by the forsterite-forming reactions 5 and 6. Tremolite formed from talc + calcite (reaction 1) at XCO₂ \approx 0.5 or from quartz and dolomite (reaction 2) at XCO₂ \approx 0.5. However, taking into account that tremolite contains Al, Na, and K in its structure, these elements may have been derived from detrital plagioclase and muscovite as suggested by Kretz (1980). There is evidence of the occurrence of forsterite in marbles. Forsterite can be the result of the presence of silica in the protolith. However, as quartz is incompatible with forsterite, it could not have been part of the precursor assemblage. Hence it is more likely that forsterite, in the presence of calcite, dolomite and diopside, grew by a reaction, such as: diopside + dolomite \rightarrow forsterite + calcite + CO₂. Diopside has probably formed from tremolite via reactions 4, 7 or 8, with Al, Na, K, and Fe derived from tremolite and, alternatively, it can be formed directly from dolomite by reaction 3, which appears to be responsible for the occurrence of pyroxene-rich assemblages. Ti-clinohumite can be preserved within calcite, which isolated Ti-clinohumite from ulterior retrogradation and allowed its preservation. On the other hand, Ti-clinohumite, clinocllore and muscovite are very often spatially associated, which indicates the supply of Al and K to the system. Several different metamorphic events on the Ciénaga Marbles have resulted in a great variety of mineral assemblages, including calcite + dolomite + Ti-clinohumite + forsterite + diopside + clinocllore + fluorapatite \pm rutile \pm muscovite \pm graphite, which corresponds to the middle amphibolite facies. Locally, retrograde antigorite after forsterite is common. However, what is the origin of Ti-clinohumite, metasomatic or metamorphic? Calcite-rich marbles are usually impermeable to fluids except for fracture-controlled fluid infiltration (Holness and Graham, 1991). Ti-clinohumite-bearing assemblages at the Ciénaga marbles are in calcite-rich domains and hence support the fact that they were affected by fracture-controlled fluid infiltration. Ti-clinohumite that occurs in the Ciénaga marbles

is associated with calcite, dolomite, forsterite, diopside, clinocllore, muscovite, rutile and fluorapatite. Antigorite forms pseudomorphs after forsterite and diopside. Alkali amphibole, which is a common phase in marbles, has not been found so far in association with Ti-clinohumite in the study area. Eventually, Ti-clinohumite may be a reaction product of preexisting forsterite, and, therefore, based on textural evidence and mineral assemblages, we suggest that Ti-clinohumite can grow by a reaction such as forsterite + dolomite + TiO₂ + H₂O \rightarrow Ti-clinohumite + calcite + CO₂. It is obvious from the compositions of these minerals that the replacement of forsterite by Ti-clinohumite implies the incorporation of Ti, F, and OH in the forsterite. Ti-clinohumite is the only phase in the forsterite-rich layers that can accommodate significant amounts of Ti and F (Chattopadhyay et al., 2009), consequently, the presence of F has a strong effect in increasing the stability of Ti-clinohumite (Rice, 1980). Because Ti-clinohumite preferentially accommodates F rather than OH, the presence of F stabilizes Ti-clinohumite (Stalder and Ulmer, 2001). The origin of Ti-clinohumite with presence of F can be attributed to a metasomatic process resulting from the external influx of F-bearing fluids or to internal buffering during metamorphism (Satish-Kumar and Niim, 1998). According to Moore and Kerriek (1976), metasomatism is normally the process operating in contact aureoles, where granodioritic intrusions inject fluids into the impure marbles causing the formation of Ti-clinohumite with presence of F. However, Rice (1980) stated that it is possible that all marbles that contain this mineral have not resulted from metasomatic introduction of F and its concentration can result from high partitioning of F into hydrous minerals. If the marbles were infiltrated by aqueous F-bearing fluids from unconnected granitoids, then the oxygen isotopes should preserve the isotopic signatures (Satish-Kumar and Niim, 1998). The origin of F in Ti-clinohumite can be also attributed to the isochemical reactions involving (OH-F) silicates such as amphiboles (tremolite), which are abundant in the Ciénaga marbles. However, it can be also associated with the occurrence of fluorapatite. Rice (1980) attributed to the partitioning of F into hydrous silicates relative to H₂O-CO₂ fluids, although this is not probably due to the presence of H₂O-rich fluids that have strongly controlled the formation of Ti-clinohumite. However, we consider that evidence of products of retrograde hydration metamorphism can be found in all these rock types, which is revealed by the occurrence of antigorite from forsterite and occasionally from diopside and Ti-clinohumite from forsterite. However, the chemical reactions described above can take place in response to an increase in the activity of H₂O relative to that of CO₂ and a decrease in temperature.

What is the role that extra components (e.g., F, Ti, Al, Fe) play in the mineralogy of marbles in the system CaO-FeO-MgO-Al₂O₃-SiO₂-TiO₂-H₂O-CO₂ (CFMAST-HC)? According to Bucher and Frey (1994), metamorphic fluids often have a small partial pressure of hydrofluoric acid (HF), and the replacement of hydroxyl groups by fluorine (F(OH)-1 exchange) rapidly decrease with increasing X_{Fe}. However, additional exchange components operating in Ti-clinohumite, such as H₂MgTi-1 and FeMg-1, are thus potentially important in determining its stability (Engi and Lindsley, 1980). Ti-clinohumite (low PHF), a mineral of the humite group, formed in forsterite marbles and may be stabilized by the presence of Ti (probably as a result of the formation of titanite reaction rims around rutile). The presence of Al in marbles promoted the formation of several minerals, such as clinocllore, epidote-group minerals, garnet, muscovite, actinolite and tremolite distributed in different reaction zones of marbles. However, a detailed study of these reactions zones is currently under study by Castellanos and co-workers (personal communication). The formation of Ti-clinohumite suggests that solutions were reduced in F. This mineral occurs in calc-silicate marbles with no ultrabasic rocks occurring either as enclaves or as discrete bodies in the vicinity. However, comparisons between Ti-clinohumite from the Ciénaga Marbles and that found in JAC carbonatites, xenoliths in kimberlites, RGP Alpine peridotites and Archean ultramafics may carry out as shown in Figure 11, highlighting that the Ti-clinohumite analyzed in this study represents not only an almost pure in Mg but also may be considered as the most Mg-rich and TiO₂-rich varieties around the world for skarn environments. Numerous mineral reactions should take place in the calcareous rocks of the Ciénaga Marbles during metamorphism. However, there are obstacles that normally encounter in carrying out an interpretation of mineral assemblages in these petrochemical type of rocks, such as: (1) complex identification of reaction textures; (2) primary or secondary nature of dolomite and quartz sometimes is unclear; (3) a gaseous phase may not be present and molecules of H₂O and CO₂ and other relatively volatile constituents may be concentrated in grain-boundaries; (4) a mineral is not normally a “pure” substance and therefore one or more compositional variables must be considered in addition to variation in the concentration or activity of H₂O and CO₂. Nonetheless, Figure 14 shows a preliminary model of the metasomatic process that probably affected the Ciénaga Marbles, which include the following steps: (1) H₂O-rich fluid by the dehydration of surrounding pelitic schists infiltrated by fractures and discontinuities into carbonate layers; (2) infiltrated H₂O-rich fluid decreased decarbonization temperatures, promoting decarbonization reactions in carbonate layers; (3) H₂O-rich fluid carried several chemical elements.

Conclusions

Calcite-dolomite marbles from the Ciénaga Marbles, Sierra Nevada de Santa Marta Massif (Colombia) contain Ti-clinohumite, which has been recognized and reported in this study. The mineral assemblage including the

presence of Ti-clinohumite within marble layers may be attributed to prograde reactions from impure dolomitic limestones. The skarn-type mineralogy of these marbles can be modeled in the system CMAST-HC. The formation of wollastonite by the interaction of marble is a very important key to consider the influence of H₂O-rich fluids. The H₂O released from the dehydration of pelitic schists probably infiltrated the calcareous rocks promoting decarbonization, which can explain the transformation of forsterite to Ti-clinohumite. Infiltration may have been the dominant mechanism during contact metamorphism, with H₂O-rich fluids derived from the crystallization of a granodiorite intrusion penetrating calcareous rocks in the contact aureole giving rise to a skarn-type mineralogy and the formation of Ti-clinohumite. The extra components (e.g., F, Ti, Al, Fe) play a role in the mineralogy of marbles in the system CFMAST-HC. Several exchange components (F(OH)-1, H₂MgTi-1 and FeMg-1) operate in Ti-clinohumite. It may be stabilized by the presence of Ti (probably as a result of the formation of titanite reaction rims around rutile). The replacement of forsterite by Ti-clinohumite implies the incorporation of Ti, F, and OH in the forsterite. Because Ti-clinohumite preferentially accommodates F rather than OH, the presence of F stabilizes Ti-clinohumite but it is necessary a very few amount of this element in the fluid or in the chemical system. The origin of Ti-clinohumite with the presence of F can be attributed to a metasomatic process resulting from the external influx of F-bearing fluids or to internal buffering during metamorphism. The origin of F in Ti-clinohumite can be also attributed to the isochemical reactions involving (OH-F) silicates such as amphiboles (tremolite). Field and petrologic evidence (occurrence of Ti-clinohumite and wollastonite, and mineral assemblages calcite + quartz + diopside, calcite + diopside + wollastonite and quartz + diopside + wollastonite) reveals that Ti-clinohumite can be developed due to infiltration of H₂O-rich fluids within forsterite-rich layers in marbles probably driven by channeling along fractures and grain boundaries.

Acknowledgments

We are grateful to L. Mantilla for guiding a fieldwork in the study area where the Ti-clinohumite-bearing marble was collected. Discussions with him aided our understanding of the Ciénaga skarn geology. Authors also thank geologist H. Cotes for providing us support to visit marble quarries. We thank laboratory facilities and their technical personnel of the School of Geology (Universidad Industrial de Santander) and Geology Program (Universidad de Pamplona). Thanks to the Laboratory of Microscopy of the Guatiguará Technological Park and its professional staff for assistance with SEM data acquisition. The manuscript was greatly improved based on the critical and helpful reviews and comments by anonymous reviewers. We are most grateful to the people and institutions mentioned earlier for support.

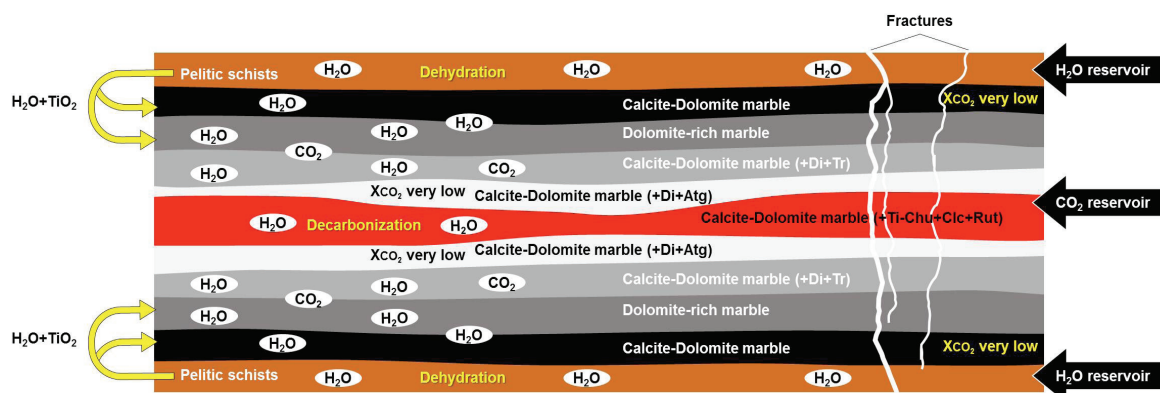


Figure 14. Schematic illustration showing the Ciénaga Marbles metasomatism (adapted and modified after Ogasawara, 2014).

References

- Ague J., 2003. Fluid infiltration and transport of major, minor, and trace elements during regional metamorphism of carbonate rocks, Wepawaug Schist, Connecticut, USA. *American Journal of Science* 303, 753-816.
- Aoki K., Fujino K., and Akaogi M., 1976. Titanochondrodite and titanoclinohumite derived from the upper mantle in the Buell Park kimberlite, Arizona, USA. *Contributions to Mineralogy and Petrology* 56, 243-253.
- Bayona G.A., Lamus-Ochoa F., Cardona A., Jaramillo C.A., Montes C., and Tcheguilakova N., 2007. Procesos orogénicos del Paleoceno para la cuenca de Ranchería (Guajira, Colombia) y áreas adyacentes definidos por análisis de procedencia. *Geología Colombiana* 32, 21-46.
- Bucher K., and Frey M., 1994. *Petrogenesis of Metamorphic Rocks*, sixth ed., Complete Revision of Winkler's Textbook, 318p.
- Cardona A., Cordani U.G., and MacDonald W.D., 2006. Tectonic correlations of pre - Mesozoic crust from the northern termination of the Colombian Andes, Caribbean region. *Journal of South American Earth Sciences* 21(4), 337-354.
- Cardona A., Valencia V., Bustamante C., García-Casco A., Ojeda G., Ruiz J., Saldarriaga M., and Weber M., 2010. Tectonomagmatic setting and provenance of the Santa Marta Schists, northern Colombia: Insights on the growth and approach of Cretaceous Caribbean oceanic terranes to the South American continent. *Journal of South American Earth Sciences* 29(4), 784-804.
- Castellanos O.M., Mantilla L.C., Ríos C.A., and Cotes H., 2013. Primer reporte de una mineralogía tipo "skarn" en los Mármoles de Ciénaga (Macizo de Santa Marta, Colombia): Implicaciones metalogénicas. XIV Congreso Colombiano de Geología y Primer Simposio de Exploradores, Julio 31 - Agosto 2 de 2013, Bogotá, D.C., Colombia.
- Castellanos O.M., Ríos C.A., and Mantilla L.C. Occurrence of a skarn-type mineralogy recognized in the "Ciénaga Marbles", NW foothills of the Santa Marta Massif (Colombia). Under review in *DYNA*.
- Chattopadhyay N., Sengupta P., and Mukhopadhyay D., 2009. Reaction textures in a suite of clinohumite - forsterite bearing marbles from parts of the Grenvillian South Delhi Fold Belt, India: Evidence of Ti mobility during regional metamorphism. EGU General Assembly 2009, held 19-24 April, 2009, Vienna, Austria <http://meetings.copernicus.org/egu2009>, p.3221.
- Connolly J.A.D., and Trommsdorff V., 1991. Petrogenetic grids for metacarbonate rocks: pressure-temperature phase-diagram projection for mixed-volatile systems. *Contributions to Mineralogy and Petrology* 108(1-2), 93-105.
- Cordani U.G., Cardona A., Jiménez D.M., Liu D., and Nutran A.P., 2005. Geochronology of Proterozoic basement inliers in the Colombian Andes: tectonic history of remnants of a fragmented Grenville belt. In: Vaughan A.P.M., Leat P.T., Pankhurst R.J. (eds), 2005. *Terrane Processes at the Margins of Gondwana*. Geological Society of London, Special Publications 246, 329-346.
- Doolan B.L., 1970. The structure and metamorphism of the Santa Marta area Colombia, South America. Ph.D. Dissertation, N.Y. State Univ., Binghamton, N.Y., 200p.
- Dymek R.F., Boak J.L., and Brothers S.C., 1988. Titanian chondrodite-and titanian clinohumite-bearing metadunite from the 3800 Ma Isua supracrustal belt, West Greenland: chemistry, petrology, and origin. *American Mineralogist* 73, 547-558.
- Engi M., and Lindsley D.H., 1980. Stability of Titanian Clinohumite: Experiments and Thermodynamic Analysis. *Contributions to Mineralogy and Petrology* 72, 415-424.
- Ferry J.M., 2000. Patterns of mineral occurrence in metamorphic rocks. *American Mineralogist* 85, 1573-1588.
- Ferry J.M., Wing B.A., and Rumble III D., 2001. Formation of Wollastonite by Chemically Reactive Fluid Flow During Contact Metamorphism, Mt. Morrison Pendant, Sierra Nevada, California, USA. *Journal of Petrology* 42, 1705-1728.
- Fujino K., and Takeuchi Y., 1978. Crystal chemistry of titanian chondrodite and titanian clinohumite of high pressure origin. *American Mineralogist* 63, 535-543.
- Gaspar J.C., 1992. Titanian clinohumite in the carbonatites of the Jacupiranga Complex, Brazil: Mineral chemistry and comparison with titanian clinohumite from other environments. *American Mineralogist* 77, 168-178.
- Hernández M., 2003. Geología de las planchas 11 Santa Marta y 18 Ciénaga, escala 1:100.000. Memoria Explicativa. INGEOMINAS. Bogotá.
- Hernández M., and Maldonado I., 1999. Geología de la Plancha 18 Ciénaga, escala 1:100.000. INGEOMINAS. Bogotá.
- Holness M.B., and Graham C.M., 1991. Equilibrium dihedral angles in the system H₂O-CO₂-NaCl-calcite, and implications for fluid flow during metamorphism. *Contributions to Mineralogy and Petrology* 108, 368-383.
- Kretz R., 1980. Occurrence, Mineral Chemistry, and Metamorphism of Precambrian Carbonate Rocks in a Portion of the Grenville Province. *Journal of Petrology* 21(3), 73-620.
- Kretz R., 1983. Symbols for rock-forming minerals. *American Mineralogist* 68, 277-279.
- Siivola J. and Schmid R., 2007. Recommendations by the IUGS Subcommission on the Systematics of Metamorphic Rocks: List of mineral abbreviations. Web version 01.02.2007. (http://www.bgs.ac.uk/scmr/docs/papers/paper_12.pdf) IUGS Commission on the Systematics in Petrology.
- MacDonald W.D., Doolan B.L., and Cordani U.G., 1971. Cretaceous-Early Tertiary Metamorphic K-Ar Age Values Front South Caribbean. *Geological Society of America Bulletin* 82, 1381-1388.
- McGetehin T.R., Silver L.T., and Chodos A.A., 1970. Titanoclinohumite: A possible mineralogical site for water in the upper mantle. *Journal of Geophysical Research* 75(2), 255-259.
- Moore J.N., and Kerriek D.M., 1976. Equilibria in siliceous dolomites of the Alta aureole, Utah. *American Journal of Science* 276, 502-524.
- Moreno-Sánchez M., and Pardo-Trujillo A., 2003. Stratigraphical and sedimentological constraints on western Colombia: Implications on the evolution of the Caribbean plate. In: Bartolini C., Buffler R.T., and Blickwede J., eds., *The Circum-Gulf of Mexico and the Caribbean: Hydrocarbon habitats, basin formation, and plate tectonics: AAPG Memoir* 79, p. 891-924.
- Muko A., Yoshioka N., Ogasawara Y., Zhu Y.F., and Liou J.G., 2001. Petrology and mineral chemistry of Ti-clinohumite-bearing garnet rock from Kokchetav ultrahigh-pressure belt. *Fluid/Slab/Mantle Interactions and Ultrahigh-P Minerals, UHPM Workshop*, Waseda University, Tokyo, pp. 190-193.
- Ogasawara Y., 2014. Titanite Stability in UHP Metacarbonate Rocks from the Kokchetav Massif, Northern Kazakhstan. *Gakujutsu Kenkyu (Academic Studies and Scientific Research) Natural Science* 62, 11-31.
- Okay A.I., 1994. Sapphirine and Ti-clinohumite in ultra-high-pressure garnet - pyroxenite and eclogite from Dabie Shan, China. *Contributions to Mineralogy and Petrology* 116, 145-155.
- Ordoñez O., Pimentel M.M., and De Moraes R., 2002. Granulitas de Los Mangos: un fragmento grenvilliano en la parte SE de la Sierra Nevada de Santa Marta. *Revista Academia Colombiana de Ciencias* 26, 169-179.
- Rabe E., 1977. Zur Stratigraphie des Ostandinen Raumes von Kolumbien I: Die Abfolge Devon bis Perm der Ost-Kordillere Nördlich von Bucaramanga; II: Conodonten des jungeren Paläozoikums der Ost-Kordillere Sierra Nevada de Santa Marta und der Sierra de Perijil. *Giessner Geologische Schriften*, No. 11, 1-95.
- Restrepo-Pace P.A., Ruiz J., Gehrels G., and Cosca M., 1997. Geochronology and Nd isotopic data of Grenville-age rocks in the Colombian Andes: new constraints for Late Proterozoic-Early Paleozoic paleocontinental reconstructions of the Americas. *Earth and Planetary Science Letters* 150, 427-441.
- Rice J.M., 1980. Phase equilibria involving humite minerals in impure dolomitic limestones, Part I.

- Calculated stability of clinohumite. *Contributions to Mineralogy and Petrology* 71, 219-235.
- Sánchez-Vizcaino V.L., Trommsdorff V., Gómez-Pugnaire M.T., Garrido C.J., Müntener O., and Connolly J.A.D., 2005. Petrology of titanian clinohumite and olivine at the high-pressure breakdown of antigorite serpentinite to chlorite harzburgite (Almirez Massif, Spain). *Contributions to Mineralogy and Petrology* 149, 627-646.
- Satish-Kumar M., and Niim M., 1998. Fluorine-rich clinohumite from Ambasamudram marbles, Southern India: mineralogical and preliminary FTIR spectroscopic characterization. *Mineralogical Magazine* 62(4), 509-519.
- Scambelluri M., and Rampone E., 1999. Mg-metasomatism of oceanic gabbros and its control on Ti-clinohumite formation during eclogitization. *Contributions to Mineralogy and Petrology* 135, 1-17.
- Spear F., 1993. *Metamorphic phase equilibria and pressure-temperature-time paths*, Monograph Series, Mineralogical Society of America, Washington, DC, 799pp.
- Stalder R., and Ulmer P., 2001. Phase relations of a serpentinite composition between 5 and 14 GPa: significance of clinohumite and phase E as water carriers into the transition zone. *Contributions to Mineralogy and Petrology* 140, 670-679.
- Trommsdorff V., and Evans B.W., 1980. Titanian hydroxyl-clinohumite: Formation and breakdown in antigorite rocks (Malenco, Italy). *Contributions to Mineralogy and Petrology* 72, 229-242.
- Tschanz C.M., Marvin R.F., and Cruz B., 1969. Geology of the Sierra Nevada de Santa Marta (Colombia) - Informe 1829. INGEOMINAS, Bogotá.
- Tschanz C.M., Jimeno A., and Cruz J., 1970. Recursos Minerales de la Sierra Nevada de Santa Marta. *Boletín Geológico INGEOMINAS XVIII*(1), 1-55.
- Tschanz C.M., Marvin R.F., Cruz B. J., Mehnert H.H., Cebula G.T., 1974. Geologic Evolution of the Sierra Nevada de Santa Marta, Northeastern Colombia. *Geological Society of America Bulletin* 85, 273-284.
- Whitney D.L., and Evans B.W., 2010. Abbreviations for names of rock-forming minerals. *American Mineralogist* 95, 185-187.
- Winter J.D., 2001. *An introduction to igneous and metamorphic petrology*. Upper Saddle River, NJ, Prentice Hall, 697pp.
- Yang J.J., Godard G., Kienast J.R., Lu Y., and Sun J., 1993. Ultrahigh-pressure (60 kbar) magnesite-bearing garnet peridotites from northeastern Jiangsu, China. *Journal of Geology* 101, 541-554.
- Yang J.J., 2003. Titanian clinohumite-garnet-pyroxene rock from the Su-Lu UHP metamorphic terrane, China: chemical evolution and tectonic implications. *Lithos* 70, 359-379.
- Zhang R.Y., Liou J.G., and Cong B.L., 1995. Talc-, magnesite- and Ti-clinohumite-bearing ultrahigh-pressure meta-mafic and ultramafic complex in the Dabie Mountains, China. *Journal of Petrology* 36, 1011-1037.
- <http://www.sfu.ca/~marshall/sem/mineral.htm> Mineral Energy Dispersive Spectra (EDS) Consulted on 15 December , 2013.